American Mineralogist, Volume 80, pages 1–8, 1995

Equation of state, bonding character, and phase transition of cubanite, $CuFe_2S_3$, studied from 0 to 5 GPa

CATHERINE A. MCCAMMON
Bayerisches Geoinstitut, Universität Bayreuth, D-95440 Bayreuth, Germany

ABSTRACT

An in-situ study of cubanite, $CuFe_2S_3$, was performed in a diamond-anvil cell using Mössbauer spectroscopy and energy-dispersive X-ray diffraction at room temperature and pressures up to 5 GPa. Mössbauer spectra of orthorhombic cubanite show a single Fe site with rapid electron transfer between Fe^{2+} and Fe^{3+}, a hyperfine magnetic field that is relatively insensitive to pressure, and a center shift that decreases with pressure because of increasing covalency. A phase transition occurs above 3.3 GPa that involves a change from the orthorhombic cubanite structure to a derivative of the hexagonal NiAs (B8) structure, with a zero-pressure volume decrease of 29%. The large difference in volume is caused by a change from tetrahedral to octahedral coordination and a significant shortening of metal-metal bonds. Volume-compression data were fitted to a second-order Birch-Murnaghan equation of state ($K_0' = 4$) with the results $K_0 = 64 \pm 3$ GPa (orthorhombic phase) and $K_0 = 157 \pm 16$ GPa (high-pressure phase). Mössbauer data of the high-pressure phase indicate a single Fe site with no magnetic ordering and a valence intermediate between Fe^{2+} and Fe^{3+}. Consideration of likely ordering patterns in the high-pressure phase indicates that localized electron transfer could occur along face-shared pairs of Fe octahedra, and extended electron delocalization could occur along paths formed by face- and edge-shared octahedra.

INTRODUCTION

The crystal structure of cubanite, $CuFe_2S_3$, is orthorhombic and is made up of coordination tetrahedra arranged in wurtzite-like slabs parallel to (010) (Fig. 1). The valence of Cu is +1, which implies that Fe occurs as Fe^{2+} and Fe^{3+} in pairs of edge-shared tetrahedra. Neutron diffraction, single-crystal X-ray diffraction, and Mössbauer spectroscopy data, however, show that the two Fe sites are identical; this has been interpreted to indicate rapid electron transfer between Fe^{2+} and Fe^{3+} (see McCammon et al., 1992, and references therein). High-pressure single-crystal X-ray diffraction experiments to 3.6 GPa have shown that the principal response of the cubanite crystal structure to increased pressure is a dramatic shortening of Cu-S bonds, resulting in an unusually low bulk modulus (McCammon et al., 1992). The mean Fe-S distance remains virtually unchanged, however, and the crystal structure accommodates the differential compression of Cu-S and Fe-S bonds by a significant tilting of tetrahedra.

Miyamoto et al. (1980) reported a dense phase of cubanite in experimental products quenched from 200 °C and pressures >4 GPa that could be indexed according to the troilite (FeS) structure. The density change is unusually high: the high-pressure phase is approximately 28% denser than the orthorhombic cubanite phase. No mechanism for the phase transition has been given, although the high-density change would suggest that an electronic change accompanies the structural transition. The nature of the high-pressure phase is of great interest because it is isostructural with FeS, a possible component of the Earth's outer core. Although FeS only remains in a NiAs-related structure to 6.7 GPa, it is important to understand the factors that stabilize $CuFe_2S_3$ in the same structure at a significantly higher density.

To characterize the behavior of cubanite at high pressure, a combined in-situ X-ray diffraction and Mössbauer spectroscopy experiment was undertaken. The goals were (1) to obtain information on the electronic structure of Fe for correlation with results from the previous structural study (McCammon et al., 1992) and (2) to observe if the high-pressure phase of cubanite could be obtained at room temperature, and, if so, to characterize the nature of the transition.

EXPERIMENTAL METHODS

A specimen of cubanite was supplied by J. Nagel, M. Y. Williams Geological Sciences Museum, University of British Columbia. X-ray diffraction measurements showed that the sample was a single phase, with cell parameters in agreement with published values (Fleet, 1970; Szymanski, 1974; McCammon et al., 1992). The sample was finely ground under acetone in an agate mortar for the diamond-anvil cell experiments.

Volume compression measurements were performed in a diamond-anvil cell of the Syassen-Holzapfel type (Huber et al., 1977) mounted with 0.25-carat diamonds with

0003–004X/95/0102–0001$02.00

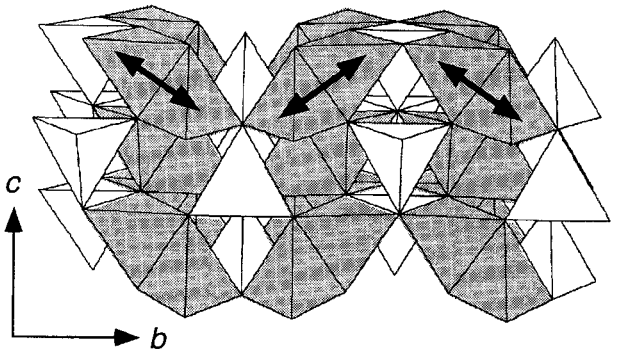

Fig. 1. Polyhedral representation of the orthorhombic cubanite structure. Cu tetrahedra are white, and Fe tetrahedra are gray. Arrows indicate the direction of rapid electron transfer.

culet diameters of 1.0 mm. A stainless steel gasket 250 μm thick (preindented to 150 μm thick) with a hole 300 μm in diameter was used to contain the sample. Powdered cubanite was pressed into a disk approximately 50 μm thick and 250 μm in diameter and mounted in the gasket hole with small ruby grains ($\sim$10 μm) for pressure calibration. A 4:1 methanol-to-ethanol mixture was used as a pressure-transmitting medium to maintain hydrostatic conditions, and pressure was measured both before and after the X-ray experiments using the ruby-fluorescence technique with the wavelength-pressure relation of Mao et al. (1986). The diamond-anvil cell was mounted on a conventional X-ray generator with a fine-focus W tube in fine-focus geometry with a collimator 100 μm in diameter. Cubanite data were collected at each pressure over approximately 24 h. Energy values were converted to d values using the Bragg equation with a Bragg angle of 5.976° (determined using an Ag calibration standard).

Mössbauer data were collected at high pressure using a modified Merrill-Bassett diamond-anvil cell (Merrill and Bassett, 1974) mounted with 0.125-carat diamonds with culet diameters of 1.0 mm. A W gasket 250 μm thick (preindented to 150 μm) with a hole 300 μm in diameter provided collimation for the γ radiation. The gasket hole was filled completely with powdered cubanite, then 4:1 methanol-to-ethanol liquid was added, along with small ruby grains ($\sim$10 μm) for pressure calibration. The diamond-anvil cell was mounted in a custom cryostat with the base of the bottom diamond at a distance of approximately 1 mm from the radioactive source. Further description of the apparatus is given in McCammon (1992). Mössbauer spectra were collected at each pressure over time periods ranging from 4 to 8 d.

Mössbauer spectra were recorded in transmission mode on a constant acceleration Mössbauer spectrometer with a nominal 50-mCi ^{57}Co source in a 6-μm Rh matrix (room pressure) and a nominal 20-mCi high specific-activity source (2 Ci/cm^2) in a 12-μm Rh matrix (high pressure). The velocity scale was calibrated relative to 25 μm α-Fe foil using the positions certified for National Bureau of Standards standard reference material 1541. Room-temperature line widths for the outer lines of α-Fe were 0.28 mm/s for the conventional source and 0.38 mm/s for the high specific-activity source. Mössbauer samples for diamond-anvil cell experiments are normally synthesized with enriched ^{57}Fe to improve the signal to noise ratio; however no successful methods of cubanite synthesis in the laboratory have been reported. The density of Fe in the room-pressure absorber was 5 mg of Fe per squared centimeter and in the high-pressure experiments was estimated to be 8 mg of Fe per squared centimeter. Mössbauer spectra were fitted to Lorentzian line shapes using the commercially available fitting program Normos written by R. A. Brand (distributed by Wissenschaftliche Electronik GmbH, Germany).

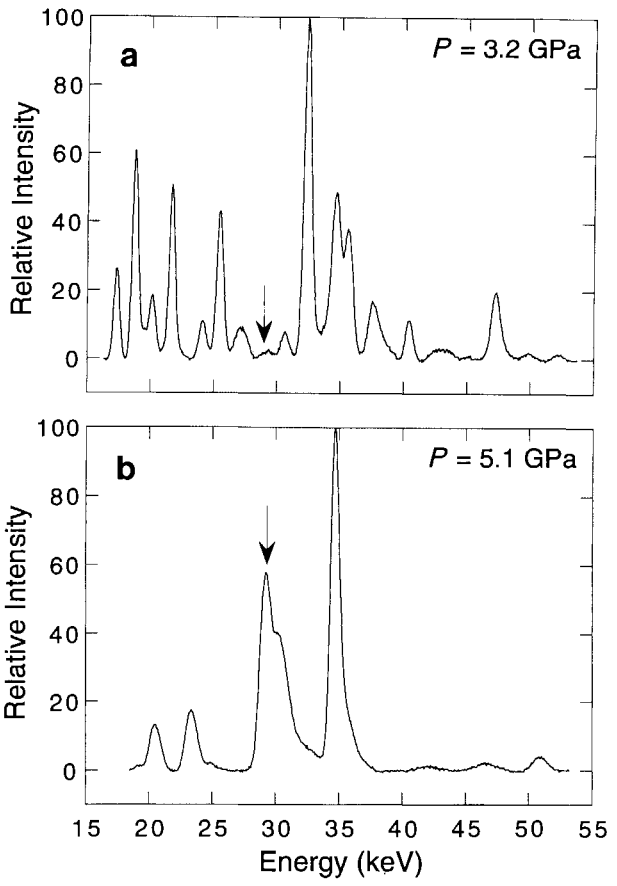

Fig. 2. Energy-dispersive X-ray diffraction spectrum for (**a**) orthorhombic and (**b**) hexagonal cubanite. The arrows indicate peaks from gasket diffraction.

Results

A typical X-ray diffraction pattern of the orthorhombic phase is illustrated in Figure 2a. The diffraction data were analyzed by fitting Gaussian line shapes to determine peak positions after base-line removal by fitting to a cubic spline curve. Peaks were indexed according to intensity data from single-crystal experiments (McCammon et al., 1992), and refinements were performed to determine unit-cell

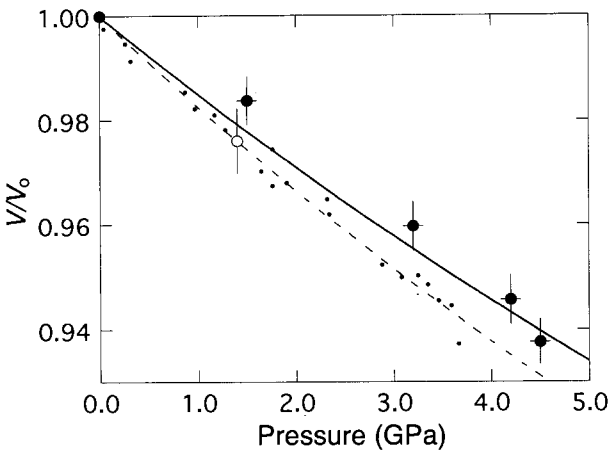

Fig. 3. Comparison of volume compression data from the present data (large circles) and single-crystal experiments of McCammon et al. (1992) (small circles). The large solid circles refer to data collected on the compression cycle, and the large open circle refers to a datum collected during decompression. The lines indicate a second-order Birch-Murnaghan equation of state with the parameters given in Table 4.

parameters. An average of ten single reflection peaks were used from each spectrum to determine cell parameters. The results are reproducible; values from different d values differ by no more than 0.2%, and the volume calculated from the spectrum at atmospheric pressure agrees with previous data in the literature. The unit-cell parameters are listed in Table 1, and the volume compression of the orthorhombic phase is plotted in Figure 3, along with single-crystal data previously reported by McCammon et al. (1992). The polycrystalline data indicate a higher bulk modulus than the single-crystal data (see discussion below).

At 5.1 GPa the X-ray diffraction pattern of cubanite transforms to the spectrum illustrated in Figure 2b. The simplest cell that fits the d-value data is hexagonal, with $a = 3.41$ and $c = 5.11$ Å; the experimental and calculated data are listed in Table 2. The hkl values of observed lines fit the simple NiAs structure. The high-pressure phase of cubanite could have the simple NiAs structure (two cations per unit cell) if Fe and Cu atoms were distributed randomly throughout the structure. The cations occupy ordered arrangements in the orthorhombic phase, however, and it would seem unlikely that kinetic energy would be sufficient at room temperature to redistribute them. The data reported by Miyamoto et al. (1980) contain a supercell reflection that does not fit the simple NiAs structure. There is no evidence for this reflection in the present data, however, although effects such as preferred orientation and the rapid decrease of intensity at higher energies might reduce the observable intensity of supercell reflections. The present X-ray data have been analyzed assuming the simple NiAs structure, but it should be understood that the actual structure probably contains ordered cations.

Table 1. Unit-cell parameters of cubanite at room temperature and high pressure

P (GPa)	a (Å)	b (Å)	c (Å)	V(cm³/mol)	Direction
		Orthorhombic phase			
0.0001	6.432(12)	11.136(31)	6.259(8)	67.50(17)	incr
1.40(5)	6.41(2)	11.12(4)	6.14(3)	65.88(41)	decr
1.5(1)	6.415(8)	11.089(16)	6.198(5)	66.40(9)	incr
3.2(1)	6.391(12)	11.008(23)	6.115(7)	64.78(14)	incr
4.2(1)	6.306(12)	10.989(26)	6.118(8)	63.83(14)	incr
4.5(1)	6.311(4)	10.951(5)	6.082(5)	63.29(5)	incr
		Hexagonal phase			
1.40(5)	3.449(17)	—	5.096(30)	47.43(45)	decr
3.59(5)	3.426(11)	—	5.135(21)	47.17(29)	decr
5.10(5)	3.409(12)	—	5.109(25)	46.45(34)	incr

X-ray diffraction spectra were initially collected in order of increasing pressure, but after the high-pressure phase at 5.1 GPa was observed, pressure was reduced to determine the reversibility of the transition. The high-pressure phase persisted at 3.6 and 1.4 GPa, but at the latter pressure reflections corresponding to the orthorhombic phase reappeared. There is no significant difference in the volume of the orthorhombic phase before and after the transition; therefore it is reversible, but with a large hysteresis.

The Mössbauer spectrum of orthorhombic cubanite is a single six-line pattern, corresponding to Fe^{2+} and Fe^{3+} undergoing rapid electron transfer with magnetic ordering between Fe atoms (the Mössbauer effect detects a single averaged $Fe^{2.5+}$ state). The room-pressure Mössbauer spectrum is illustrated at the top of Figure 4. The data agree with previous results (Imbert and Wintenberger, 1967) and show a combined quadrupole and magnetic interaction. The spectra were fitted using the full interaction Hamiltonian to the parameters center shift (δ), hyperfine magnetic field (H), quadrupole splitting (ΔE_Q), asymmetry parameter of the electric field gradient (η), and the polar and azimuthal angles between the directions of the magnetic field and γ-ray propagation (θ and ϕ, respectively). The first two parameters (δ and H) can be determined unambiguously, but the last four parameters are related through three equations; therefore it is not always possible to determine unambiguous values (the ambiguity problem was first described by Karyagin, 1966). To determine the best-fit parameter set, ϕ was held constant at successive values while the three remaining pa-

Table 2. Comparison of observed and calculated X-ray data at $P = 5.1$ GPa for high-pressure cubanite in the simple NiAs structure

I	hkl	d_{obs} (Å)	d_{calc} (Å)
17	100	2.905	2.952
19	101	2.550	2.556
64	102	1.956	1.932
100	110	1.714	1.705
3	201	1.416	1.418
5	202	1.277	1.278
6	104	1.170	1.172

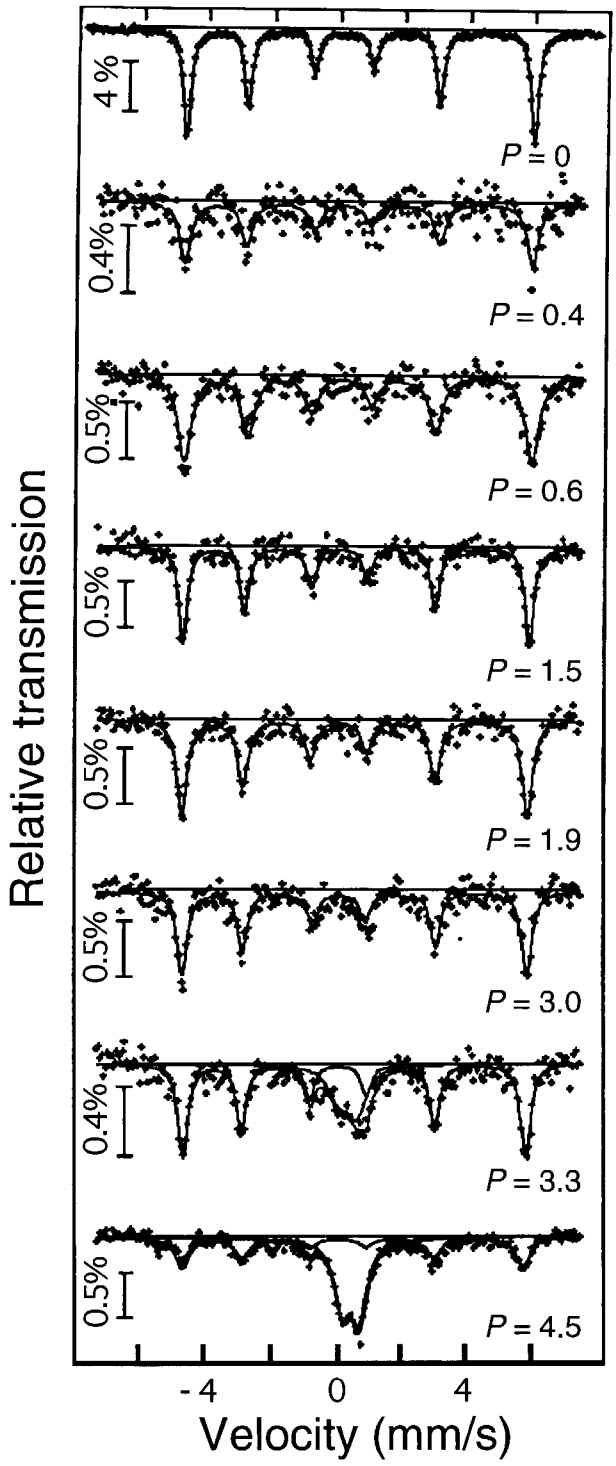

Fig. 4. Mössbauer spectra of cubanite recorded at high pressure. The top spectrum was recorded in air at room pressure, and the remainder were recorded in a diamond-anvil cell. Pressures are given in GPa.

rameters were optimized until the solution giving the lowest χ^2 was found. Then the values of ΔE_Q, η, θ, and ϕ were used as input to the secular equation for the eigenvalues to generate all other possible solutions. The range

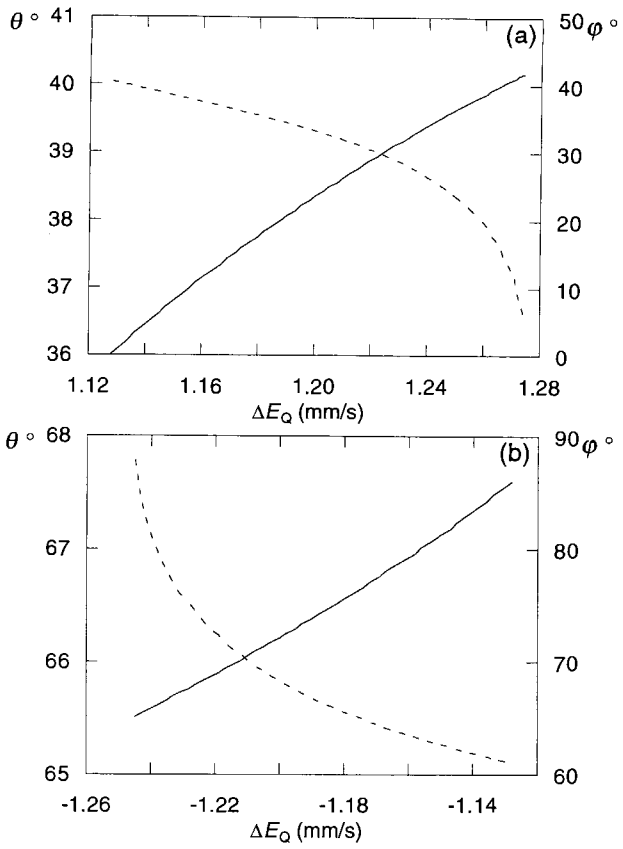

Fig. 5. Interdependence of the hyperfine parameters of orthorhombic cubanite at room pressure for positive (a) and negative (b) values of ΔE_Q. The variation of η is not shown.

of solutions is illustrated in Figure 5, where the values of θ and ϕ are plotted against ΔE_Q. The value of η (not shown) varies considerably: for positive values of ΔE_Q, η varies from 0.37 to 1.00, and for negative values it varies from 0.53 to 1.00 (the allowed values of η are from 0 to 1). The values of ΔE_Q and θ are relatively well constrained, whereas ϕ varies over nearly the entire range from 0 to 90°. The existing data do not allow a decision as to whether ΔE_Q is positive or negative, and techniques to determine the sign (e.g., recording the spectrum in an applied magnetic field above the magnetic ordering temperature) are not possible because cubanite undergoes an irreversible phase transition below the ordering temperature.

The quality of Mössbauer spectra is reduced in diamond-anvil cell experiments (Fig. 4). Spectral absorption decreases dramatically because of source thickness effects, increase in background due to X-rays from the gasket, and absorption of 14.4 keV radiation by the diamonds. Spectrum quality improves with pressure, however, probably because of an increase in recoil-free fraction. Because line positions and intensities are constrained by the eigenvalues and eigenvectors of the interaction Hamiltonian, the number of adjustable parameters in the fitting model is small; therefore it is possible to extract meaningful data from the high-pressure spectra.

TABLE 3. Mössbauer parameters of cubanite at room temperature

P (GPa)	δ^* (mm/s)	H (T)	ΔE_Q^{**} (mm/s)	η^{**}	θ^{**} (°)	Γ (mm/s)	Area (%)
Orthorhombic phase							
0.0001	0.395(1)	32.34(3)	1.272(4)	0.38(8)	40.1(3)	0.271(3)	100
0.4(1)	0.40(2)	32.0(5)	1.51(7)	0.8(6)	48.4(20)	0.41(5)	100
0.6(1)	0.41(1)	32.0(3)	1.48(6)	0.3(6)	42.2(25)	0.50(3)	100
1.5(1)	0.38(1)	31.7(2)	1.56(4)	0.7(2)	46.7(10)	0.32(2)	100
1.9(1)	0.37(1)	32.1(2)	1.30(4)	0.6(4)	43.9(10)	0.39(2)	100
3.0(1)	0.38(1)	31.7(3)	1.50(4)	0.9(4)	49.8(10)	0.36(3)	100
3.3(1)	0.36(1)	32.3(3)	0.90(5)	0.2(12)	32.3(50)	0.37(3)	71
4.5(1)	0.33(2)	32.0(5)	0.98(50)	0.3(15)	38(20)	0.53(4)	45
Hexagonal phase							
3.3(1)	0.40(6)	—	0.57(7)	—	—	0.75(10)	29
4.5(1)	0.48(2)	—	0.52(2)	—	—	0.58(5)	55

* Relative to α-Fe.
** $\phi = 10°$.

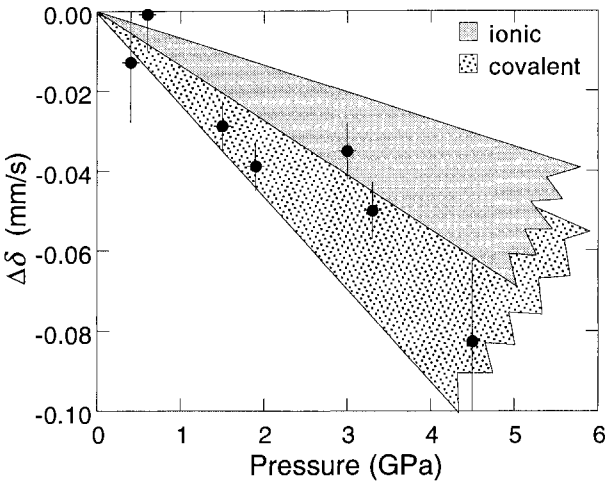

Fig. 6. Effect of pressure on the isomer shift of orthorhombic cubanite relative to the zero-pressure value. Observed ranges for ionic and covalent compounds from Drickamer et al. (1969) are included for comparison.

The spectra were fitted with the full interaction Hamiltonian with fixed ϕ; the parameters are listed in Table 3 for $\phi = 10°$.

Above 3.3 GPa a new component was observed in the Mössbauer spectra (Fig. 4). It is nonmagnetic and consists of at least two singlets or one quadrupole doublet. The simplest fitting model that gives realistic values for the hyperfine parameters is a quadrupole doublet with asymmetric line intensities: results are listed in Table 3. The area asymmetry of the quadrupole doublet is probably due to the preferred orientation of a small number of crystallites. This interpretation is consistent with the observation that component line widths are equal within experimental uncertainty. Following data collection at the highest pressure (4.5 GPa), the sample was decompressed to ambient conditions and a further Mössbauer spectrum was recorded. It indicated a complete reversion to the low-pressure magnetic phase.

Following observation of the high-pressure phase in the Mössbauer data above 3.3 GPa, the X-ray data were reexamined for evidence of the high-pressure phase. At least one line from the high-pressure phase can be clearly seen in the spectrum recorded at 4.5 GPa. The other lines are probably present but cannot be distinguished because of the overlap with lines from the orthorhombic phase. A similar situation exists for the spectrum recorded at 4.2 GPa. Since the relative intensities of phases depend on different factors for the X-ray and Mössbauer experiments, it is not unusual that the relative intensities of the orthorhombic and high-pressure phases differ in the two experiments.

Discussion

Orthorhombic phase

The center shift of orthorhombic cubanite is intermediate between values typical for Fe^{2+} and Fe^{3+} because of rapid electron transfer and the fact that the Mössbauer effect detects an averaged environment. The center shift consists of the isomer shift plus a second-order Doppler shift (SOD), and since the effect of pressure on the SOD is small for Fe compounds (Williamson, 1978), the isomer shift of cubanite can be assumed to decrease with pressure at the same rate. Two effects have been suggested for changing the s electron density at the nucleus (i.e., the isomer shift) with pressure: (1) changes in orbital occupation and (2) distortion of the wavefunctions—either compression of the s electrons or spreading out of the 3d electrons (increase in covalency) (Drickamer et al., 1969). The second factor, specifically an increase in covalency, is thought to dominate the effect of pressure on isomer shifts of ionic compounds because isomer shifts fall within a relatively narrow range and are correlated with the valence of the Fe atom. Covalent compounds show a greater range of pressure coefficients, where changes in orbital occupation are thought to dominate. These changes include transfer of electrons between the Fe 3d and 4s levels, between different Fe 3d levels, and between Fe orbitals and orbitals of the coordinating anions.

Figure 6 illustrates the variation of the center shift of cubanite with pressure compared with the range of variation for a number of ionic and covalent compounds taken from Drickamer et al. (1969). The isomer shift of orthorhombic cubanite decreases at a rate greater than that of ionic compounds, which might be attributed to the intervalence charge transfer process in cubanite. Pressure generally intensifies charge transfer bands through a lowering of the activation energy for the charge transfer process (e.g., Burns, 1993). This results in a higher electron density in the charge transfer orbitals, which lowers the effective shielding by the 3d orbitals of 3s and 4s electrons at the Fe nucleus, thereby decreasing the isomer shift. This effect is probably greater than the effect of increased covalency in lowering the isomer shift because of the effect of pressure on Fe-S and Fe-Fe distances in orthorhombic cubanite. Single-crystal experiments have shown that Fe-S distances remain approximately constant to 3.6 GPa, and, since the degree of covalency is related to the

TABLE 4. Bulk moduli calculated from volume-compression data fitted to a second-order Birch-Murnaghan equation of state

Phase	K_0 (GPa)	V_0 (cm³/mol)	Reference
Cubanite			
Ortho. (polycrystal)	64(3)	67.50(30)	this work
Ortho. (single crystal)	55(4)	67.34(47)	McCammon et al. (1992)
Hex. (polycrystal)	157(16)	47.99(68)	this work
FeS (single crystal)	65(2)	18.16(10)	King and Prewitt (1982)

cation-anion distance, there should be no significant increase in covalency. In contrast, Fe-Fe distances decrease because of the tilting of Fe tetrahedra, and so the electron density in charge transfer orbitals would therefore increase.

The magnetic hyperfine field is generally assumed to be proportional to the bulk magnetization of the material, which depends on the strength of exchange interactions and the size of magnetic moments of the atoms. Pressure can reduce the magnetic moment through an increase in covalency, which decreases the unbalanced spin density of electrons at the Fe nucleus, similar to the effect on the isomer shift. But in contrast to the isomer shift data, the magnetic hyperfine field of cubanite does not vary significantly with pressure (Table 3). This suggests that the covalency of Fe-S bonds does not significantly increase at high pressure and is consistent with the conclusion above, that the decrease in the isomer shift is caused primarily by intensification of the charge transfer process with increasing pressure.

Volume-compression data derived from the X-ray diffraction spectra were fitted to a Birch-Murnaghan equation of state (Birch, 1952, 1978), which is

$$P = 3f(1 + 2f)^{5/2}K_0\left[1 - \frac{3f}{4}(4 - K_0')\right] \quad (1)$$

in the third-order expansion where the Eulerian finite strain (f) is given by

$$f = \frac{1}{2}\left[\left(\frac{V}{V_0}\right)^{-2/3} - 1\right]. \quad (2)$$

The formulation of Jeanloz (1981) was used in which the equation of state is expressed as a series of linear equations involving the variables K_0, K_0', and V_0, enabling the best-fit values of these parameters to be determined through weighted linear least-squares regression. Initially K_0' was considered a variable parameter (third-order fit), but an F test showed that the improvement in χ^2 of a third-order fit was not statistically significant for either the orthorhombic or the hexagonal cubanite data sets; therefore K_0' was fixed to 4.0 (second-order fit). The results are listed in Table 4. For comparison, previous single-crystal results from orthorhombic cubanite (McCammon et al., 1992) and hexagonal FeS (King and Prewitt, 1982) were fitted with the same method. Although the zero-pressure volume determined for polycrystalline cubanite

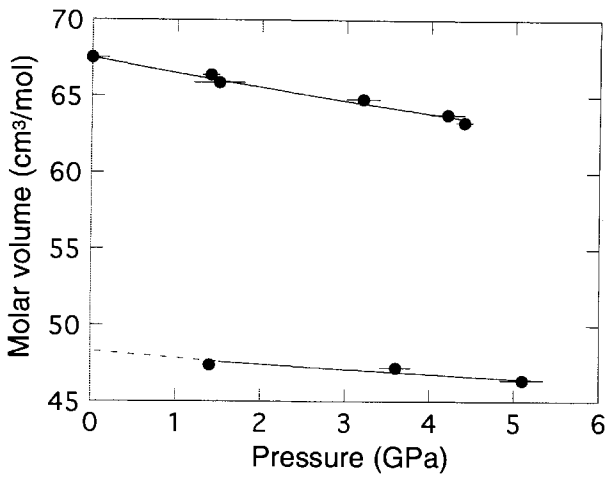

Fig. 7. Volume compression of cubanite showing the orthorhombic → hexagonal phase transition.

agrees with the value from single-crystal experiments, the bulk modulus is significantly higher. One explanation could be a systematic difference in pressure calibration, although that would appear unlikely. The single-crystal data were calibrated using two techniques, ruby fluorescence and a CaF_2 X-ray standard; both methods gave similar results. The polycrystalline data were calibrated using only ruby fluorescence, but since pressure was calibrated from the relative change in wavelength using the same relation that was used in the single-crystal experiments, it is unlikely that systematic errors could be large enough to produce the observed discrepancy (~15%). A more likely possibility is that the discrepancy is caused by a difference in microstructure between the samples. On decompression, the volume of the polycrystalline sample is equal to the volume of the single crystal (Fig. 3); that could reflect a change in microstructure after the phase transition. Since microstructure effects can either increase or decrease compressibility, it is impossible without further data to determine which data set (single crystal or polycrystalline) provides a more appropriate measure of the bulk modulus of cubanite.

Hexagonal phase

Volume-compression data from the hexagonal phase were fitted to a second-order Birch-Murnaghan equation; the results are listed in Table 4 and illustrated in Figure 7. Standard errors were calculated by propagation of uncertainties in measured quantities but are likely to underestimate the true error because of the small number of data points. The calculated zero-pressure density of the hexagonal phase is 5.67 ± 0.23 g/cm³, which is slightly greater than the value of 5.2 g/cm³ reported by Miyamoto et al. (1980). The bulk modulus of the hexagonal phase is more than twice the value for FeS, which has a similar crystal structure. This is accounted for, in part, by the smaller density of FeS (4.84 g/cm³).

The high density of the hexagonal phase can be ex-

plained by examining the mean bond lengths. Figure 8 illustrates the effect of pressure on mean M-S and M-M bond lengths in orthorhombic cubanite (taken from single-crystal data of McCammon et al., 1992) and the hexagonal phase. Errors for the latter bond lengths were estimated from differences in ionic radii of Fe and Cu cations and the maximum expected deviation from standard atomic coordinates; single-crystal orthorhombic data for Fe and Cu were averaged for comparison with the powder hexagonal data. Despite large errors, the trends illustrated in Figure 8 are clear. Fe-S bond distances increase from the orthorhombic to the hexagonal phase (Fig. 8a), but the increase is much smaller than expected for a change from tetrahedral to octahedral coordination. To examine the degree of metal-anion shortening, it is useful to explore the relation between volume and bond lengths in the NiAs structure. Assuming an ideal c/a value of $\sqrt{8/3}$, metal-anion bond distances were calculated for a cell with the same volume as the hexagonal phase and for a cell with the same volume as the orthorhombic phase. For the calculation, ideal metal and anion atomic coordinates of (0,0,0) and ($\frac{1}{3},\frac{2}{3},\frac{1}{4}$), respectively, were assumed, giving the relation $\langle M\text{-}S\rangle = (\frac{1}{3}a^2 + \frac{1}{16}c^2)^{1/2}$. The results are plotted in Figure 8a and show the large increase in metal-anion distance if there is no volume change during the transition (dashed line). When the volume change is increased to the observed value of 29%, however, there is a dramatic shortening of metal-anion bonds (dotted line).

A similar calculation can be made for the metal-metal distances, where $\langle M\text{-}M\rangle = c/2$ for the ideal c/a ratio of $\sqrt{8/3}$. In the NiAs structure the value of c/a can vary dramatically between different compounds because of metal-metal bonding or metal-metal repulsion, which decreases or increases, respectively, the observed ratio from the ideal value. The average c/a ratio for hexagonal cubanite of 1.49 is smaller than the ideal value, indicating a shortening of metal-metal distances. Figure 8b illustrates the significant compression of metal-metal bonds in the hexagonal phase (open circles) compared with a hexagonal cell with the same volume but with an ideal c/a ratio (dotted line).

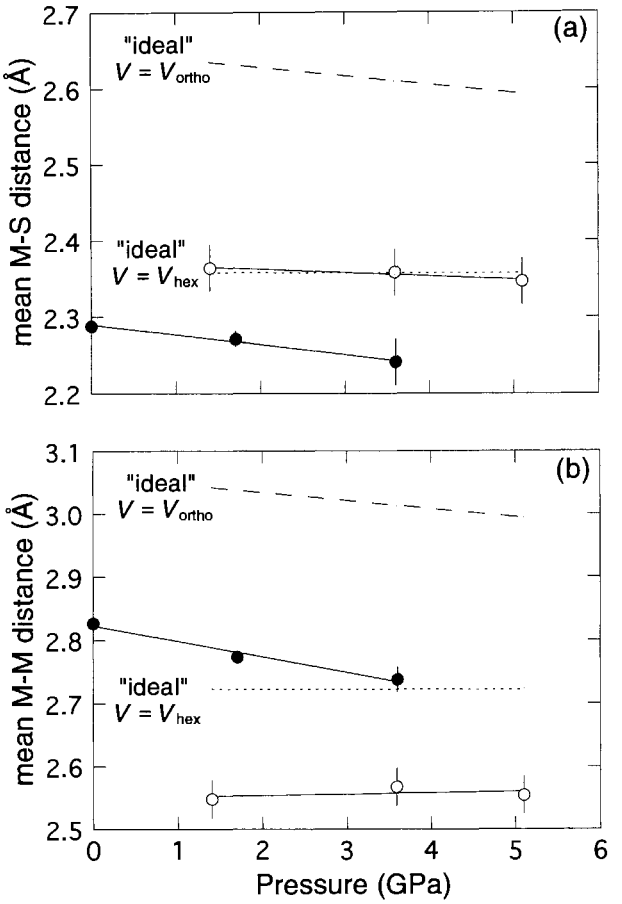

Fig. 8. Calculated Fe-S (**a**) and Fe-Fe (**b**) distances for orthorhombic cubanite (data from McCammon et al., 1992) (solid circles) and hexagonal cubanite (open circles). The dashed lines indicate the calculated Fe-S and Fe-Fe distances for an ideal hexagonal cell ($c/a = \sqrt{8/3}$) with the same volume as the orthorhombic cell (i.e., $\Delta V = 0$), and the dotted lines indicate the corresponding distances in an ideal hexagonal cell with the same volume as the observed value.

In summary, the major contributing factor to the high density of hexagonal cubanite is a large decrease in metal-anion bond length, supplemented by significant shortening of the metal-metal bonds. Both types of bond compression are likely to affect the electronic structure of Fe in hexagonal cubanite.

The Mössbauer parameters of the hexagonal phase provide information on the electronic environment of Fe. The center shift of the hexagonal phase (0.48 mm/s at 4.5 GPa) is larger than the value for orthorhombic cubanite (0.33 mm/s at 4.5 GPa), which can be accounted for by the change from tetrahedral to octahedral coordination where Fe-S bond lengths increase (greater shielding of the s electrons by the 3d electrons). The center shift of the hexagonal phase is significantly smaller than the value for FeS (0.70 mm/s at 5.2 GPa: King et al., 1978), however, despite the similar crystal structure. That suggests that the valence of Fe in hexagonal cubanite is also intermediate between Fe^{2+} and Fe^{3+}. Figure 9 illustrates the NiAs structure, which can be viewed as columns of face-shared octahedra parallel to the **c** axis, where columns are joined by their edges. Since transformation to the NiAs structure occurs at room temperature, it is likely that the ordered arrangement of cations in the orthorhombic phase is preserved. Accordingly, octahedra in Figure 9 have been shaded to indicate a likely arrangement of Cu and Fe atoms in the hexagonal phase. The Fe sites form pairs of face-shared octahedra parallel to the **c** axis; these are indicated by arrows in Figure 9 and show the direction of possible electron transfer between Fe^{2+} and Fe^{3+}. The pairs of Fe octahedra are also joined by edges, which could result in extended electron delocalization throughout the crystal structure and metallic behavior. Orthorhombic cubanite is nonmetallic (Sleight

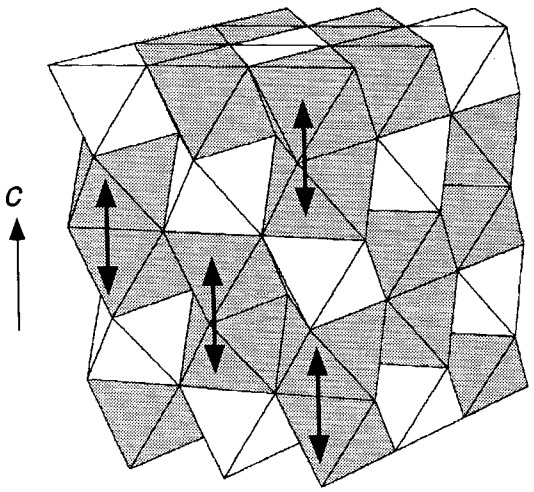

Fig. 9. Polyhedral representation of a possible arrangement of cations in hexagonal cubanite. Cu octahedra are white, and Fe octahedra are gray. Arrows indicate a possible path for electron transfer.

and Gillson, 1973), which is consistent with the restriction of electron transfer to pairs of Fe tetrahedra. This raises the possibility of a nonmetal to metal transition at high pressure, and electrical resistivity measurements are planned to investigate further the nature of the high-pressure phase.

Conclusions

Cubanite undergoes a first-order phase transition above 3.3 GPa from the orthorhombic structure to a derivative of the NiAs structure, accompanied by a zero-pressure volume change of 29%. The large difference in volume is caused by a change from tetrahedral to octahedral coordination and is supplemented by a significant shortening of metal-metal bonds. These bonds are stabilized by rapid electron transfer between Fe^{2+} and Fe^{3+} across shared octahedral faces. FeS has a similar crystal structure but is significantly less dense because Fe^{2+}-S and Fe^{2+}-Fe^{2+} distances are larger than corresponding distances in high-pressure cubanite. FeS is not stable in this structure at high pressure, however; it undergoes a transition to an as yet unknown structure above 6.7 GPa (e.g., King and Prewitt, 1982). An interesting question, therefore, is whether cubanite undergoes a similar transition at higher pressure. The answer would provide data on the ability of the Fe^{2+}-Fe^{3+} electron transfer to stabilize the NiAs-type structure and could provide insight into the 6.7-GPa phase transition in FeS, a transition that is still poorly understood.

References cited

Birch, F. (1952) Elasticity and constitution of the Earth's interior. Journal of Geophysical Research, 57, 227–286.

——— (1978) Finite strain isotherm and velocities for single-crystal and polycrystalline NaCl at high pressures and 300 K. Journal of Geophysical Research, 83, 1257–1268.

Burns, R.G. (1993) Mineralogical applications of crystal field theory (2nd edition), 551 p. Cambridge University Press, Cambridge, U.K.

Drickamer, H.G., Vaughn, R.W., and Champion, A.R. (1969) High-pressure Mössbauer resonance studies with iron-57. Accounts of Chemical Research, 2, 40–47.

Fleet, M.E. (1970) Refinement of the crystal structure of cubanite and polymorphism of $CuFe_2S_3$. Zeitschrift für Kristallographie, 132, 276–287.

Huber, G., Syassen, K., and Holzapfel, W.B. (1977) Pressure dependence of 4*f* levels in europium pentaphosphate up to 400 kbar. Physical Review B, 15, 5123–5128.

Imbert, P., and Wintenberger, M. (1967) Étude des propriétés magnétiques et des spectres d'absorption par effet Mössbauer de la cubanite et de la sternbergite. Bulletin de la Société français de Minéralogie et de Cristallographie, 90, 299–303.

Jeanloz, R. (1981) Finite-strain equation of state for high-pressure phases. Geophysical Research Letters, 8, 1219–1222.

Karyagin, S.V. (1966) Determination of the local field parameters in Mössbauer hyperfine spectra. Soviet Physics, Solid State, 8, 391–396.

King, H.E., and Prewitt, C.T. (1982) High-pressure and high-temperature polymorphism of iron sulphide (FeS). Acta Crystallographica, B38, 1877–1887.

King, H., Virgo, D., and Mao, H.K. (1978) High-pressure phase transitions in FeS, using ^{57}Fe Mössbauer spectroscopy. Carnegie Institution of Washington Year Book, 77, 830–835.

Mao, H.K., Xu, J., and Bell, P.M. (1986) Calibration of the ruby pressure gauge to 800 kbar under quasi-hydrostatic conditions. Journal of Geophysical Research, 91, 4673–4676.

McCammon, C.A. (1992) A new apparatus to conduct variable temperature high pressure Mössbauer spectroscopy. In A.K. Singh, Ed., Recent trends in high-pressure research: Proceedings of XIII AIRAPT International Conference on High Pressure Science and Technology, p. 824–826. Oxford and IBH, New Dehli, India.

McCammon, C.A., Zhang, J., Hazen, R.M., and Finger, L.W. (1992) High-pressure crystal chemistry of cubanite, $CuFe_2S_3$. American Mineralogist, 77, 937–944.

Merrill, L., and Bassett, W.A. (1974) Miniature diamond anvil pressure cell for single-crystal X-ray diffraction studies. Reviews of Scientific Instruments, 45, 290–294.

Miyamoto, M., Ishii, T., Kume, S., and Koizumi, M. (1980) A new polymorph of cubanite, $CuFe_2S_3$. Materials Research Bulletin, 15, 907–910.

Sleight, A.W., and Gillson, J.L. (1973) Electrical resistivity of cubanite: $CuFe_2S_3$. Journal of Solid State Chemistry, 8, 29–30.

Szymanski, J.T. (1974) A refinement of the structure of cubanite, $CuFe_2S_3$. Zeitschrift für Kristallographie, 140, 218–239.

Williamson, D.L. (1978) Influence of pressure on isomer shifts. In G.K. Shenoy and F.E. Wagner, Eds., Mössbauer isomer shifts, p. 317–360. North-Holland, Amsterdam.

Manuscript received March 31, 1994
Manuscript accepted August 22, 1994